GEOLOGY | THE GEOLOGICAL SOCIETY OF AMERICA®

https://doi.org/10.1130/G50094.1

Manuscript received 30 January 2022
Revised manuscript received 5 April 2022
Manuscript accepted 7 April 2022

Published online 27 May 2022

The role of flat slab subduction, ridge subduction, and tectonic inheritance in Andean deformation

Brian K. Horton[1], Tomas N. Capaldi[2] and Nicholas D. Perez[3]

[1]Institute for Geophysics and Department of Geological Sciences, Jackson School of Geosciences, University of Texas at Austin, Austin, Texas 78712, USA

[2]Department of Geoscience, University of Nevada–Las Vegas, Las Vegas, Nevada 89154, USA

[3]Department of Geology and Geophysics, College of Geosciences, Texas A&M University, College Station, Texas 77843, USA

ABSTRACT

Convergent plate boundaries show sharp variations in orogenic width and extent of intraplate deformation. Analysis of late Cenozoic contractile deformation along the Andean mountain front and adjacent foreland highlights the contrasting degrees of deformation advance toward the plate interior. The retroarc positions of the Andean topographic front (marked by frontal thrust-belt structures) and foreland deformation front (defined by isolated basement block uplifts) range from 300 to 900 km inboard of the trench axis. Over the ~8000 km arcuate length of the Andes (10°N to 55°S), four discrete maxima of inboard deformation advance are spatially co-located with the Peruvian (5°S–14°S) and Pampean (27°S–33°S) zones of flat slab subduction, the subducted Chile Ridge (45°S–48°S), and the anomalously thick Paleozoic stratigraphic wedge of Bolivia (17°S –23°S). The spatial correspondence of retroarc shortening with specific geodynamic configurations demonstrates the mechanical role of flat slab subduction, slab window development, and combined structural and stratigraphic geometries in shaping the orogenic architecture of Cordilleran margins, largely through lithospheric strengthening, weakening, and/or tectonic inheritance.

INTRODUCTION

Spatial variations in the magnitude and mode of deformation advance govern the topographic and structural framework of Andean-type orogens and their adjacent forelands. Disparate degrees of deformation advance are reflected in the arcuate trace of the topographic front—which marks the inboard penetration of the fold-thrust belt toward the craton—and in the distribution of isolated basement-involved uplifts across the flanking foreland basin (Kley et al., 1999; McGroder et al., 2015). The geodynamic controls on deformation advance and intraforeland uplift remain unclear, resulting in debate over the competing roles of flat slab subduction, ridge subduction, structural reactivation, shortening magnitude, and mantle flow (Gutscher et al., 2000; Ramos, 2005; Schellart, 2017; Bishop et al., 2018; Horton, 2018a; Schellart and Strak, 2021).

The modern Andes exhibit pronounced contrasts in the regional architecture of the retroarc fold-thrust belt and foreland. Whereas the thrust belt spans the length of the orogen, intraforeland deformation is best expressed in the Peruvian (5°S –14°S) and Pampean (27°S –33°S) segments (Fig. 1). Foreland shortening and uplift of basement blocks (such as the Sierras Pampeanas) have been widely attributed to flat slab subduction (Jordan et al., 1983; Ramos et al., 2002; Ramos and Folguera, 2009) and adopted as a global example of noncollisional intraplate deformation (Dickinson and Snyder, 1978; Ye et al., 1996; Li and Li, 2007; Yonkee and Weil, 2015; Kusky et al., 2016). Others have suggested that the preexisting structural, stratigraphic, and rheological framework of the overriding continental lithosphere exerts a first-order control on retroarc deformation (e.g., McQuarrie, 2002; Gautheron et al., 2013). From these contradictory views, the relevance of slab dynamics to the style and timing of intraforeland deformation may be regarded as essential or as grossly overstated. This is a pivotal issue because intraplate deformation has been considered a direct consequence of a shallow slab and thus routinely used to infer flat slab subduction in tectonic reconstructions of plate interactions, arc magmatism, and craton evolution (Kusky et al., 2014; Capaldi et al., 2021).

Our study compares the scope of retroarc deformation advance along the length of the Andes to varied geodynamic, structural, and stratigraphic parameters of western South America. This comparison enables assessment of flat slab subduction, ridge subduction, and tectonic inheritance in guiding deformation of the orogenic belt and adjacent foreland basin.

GEOLOGIC SETTING

Plate convergence along western South America is accommodated by subduction of oceanic lithosphere of the Nazca and Antarctic plates (Fig. 1). Spreading ridges and aseismic ridges intersect the trench in several localities. Where the Chile Ridge (Nazca-Antarctic plate boundary) meets the continent, a slab window has opened beneath the northern Patagonian Andes and retroarc foreland (Ramos, 2005; Breitsprecher and Thorkelson, 2008). Elsewhere, late Cenozoic subduction of aseismic ridges correlates spatially with flat slab subduction beneath the western Amazonian foreland of Peru and the Pampean foreland of central Argentina (Ramos et al., 2002; Bishop et al., 2018).

The western margin includes a continental forearc, magmatic arc (preferentially extinguished in zones of shallow subduction), retroarc fold-thrust belt, and foreland basin (Fig. 1). Along the margin, the Andean orogenic wedge defines a continuous belt with alternating concave and convex curvature toward the foreland (Fig. 1). Although commonly portrayed as a linear belt, the Andes show substantial variations in tectonic strike, with only ~60% of the orogen in

CITATION: Horton, B.K., Capaldi, T.N., and Perez, N.D., 2022, The role of flat slab subduction, ridge subduction, and tectonic inheritance in Andean deformation: Geology, v. 50, p. 1007–1012, https://doi.org/10.1130/G50094.1

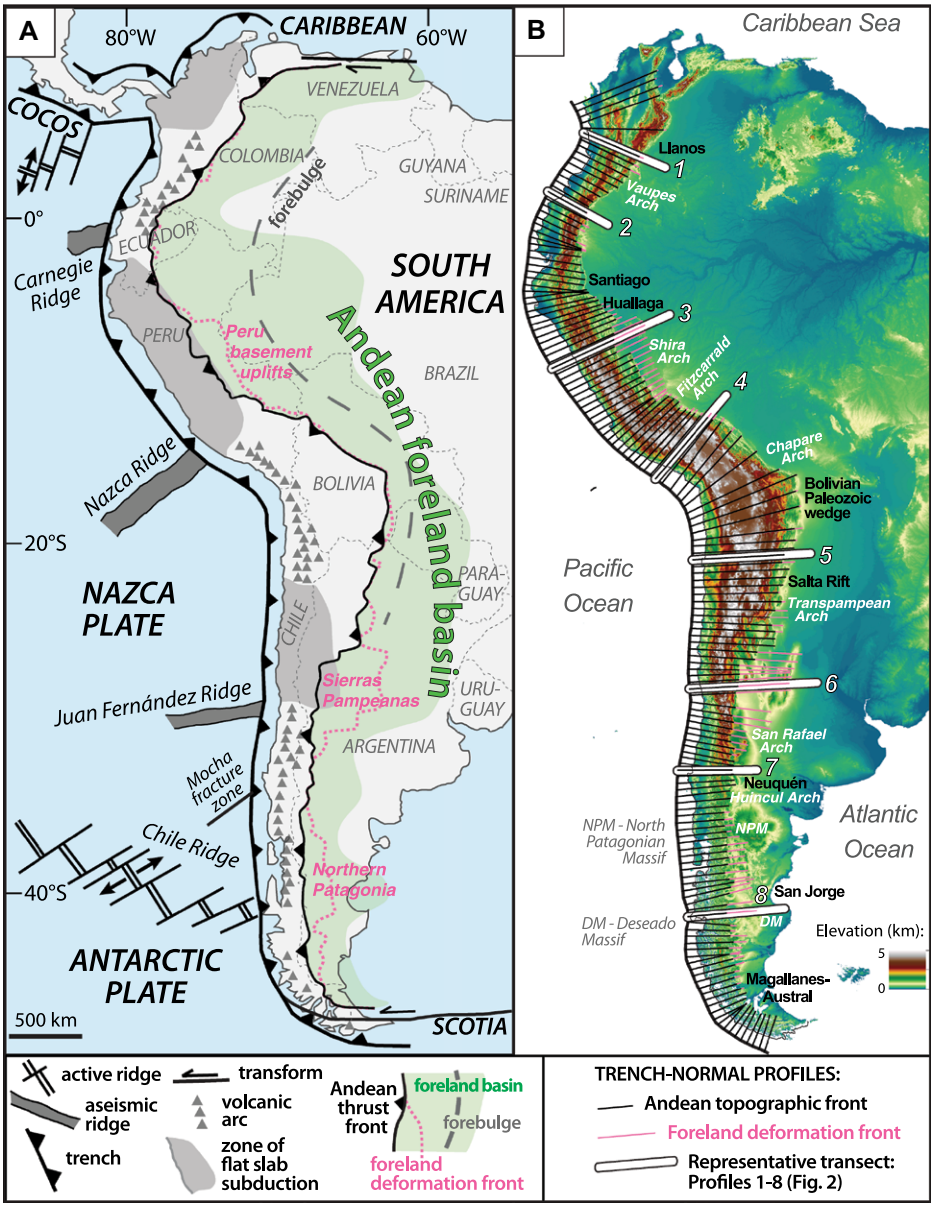

Figure 1. Tectonic map (A) and shaded topography (B) of western South America showing plate boundaries, volcanic arc, zones of flat slab subduction, basement arches (white labels), and selected basin segments (black labels). The topographic front of the Andean fold-thrust belt (black barbed line) and foreland deformation front (pink line) are derived from trench-normal profiles spaced every 50 km along the trench axis.

the 340°–025° azimuthal range (Fig. S1 in the Supplemental Material[1]). Accurate visualization of the topographic and structural framework thus requires a common geologic reference such as spatial position relative to the trench.

STRUCTURAL AND TOPOGRAPHIC CONTEXT

Compilation of late Cenozoic faults along the Andean topographic front and adjacent foreland (Proyecto Multinacional Andino, 2009; Costa et al., 2020; Styron and Pagani, 2020) enables delineation of (1) the Andean topographic front, where the Andean fold-thrust belt meets the low-relief foreland basin; and (2) the foreland deformation front, defined as the inboard limit of deformation advance (Table S1). Identification of these two critical features in maps (Fig. 1) and trench-normal cross sections (Fig. 2) reveals contrasting tectonomorphic configurations along the margin.

The topographic front coincides with the deformation front over large segments of the central (15°S –25°S) and northern (10°N–5°S) Andes. However, the deformation front is situated far inboard of the Andean mountain front in the Peruvian (5°S –14°S), Pampean (27°S –33°S), and northern Patagonian (45°S –48°S) zones of distributed foreland shortening.

The map (Fig. 1) and representative profiles (Fig. 2) show a 300–900 km orogenic width from the trench to the Andean topographic front, with the foreland deformation front demarcated by structures positioned either at the mountain front (profiles 1, 2, 4, 5, and 7) or as much as 400 km inboard of the mountain front (profiles 3, 6, and 8). Within the profiles, the Andean orogenic wedge consists of a retroarc fold-thrust belt exhibiting a systematic slope dipping toward the foreland. This integrated Andean topography is spatially distinct from isolated topographic highs delimited by basement-cored foreland uplifts in the Peruvian, Pampean, and northern Patagonian provinces (Fig. 2).

In addition to topographic discrepancies, the regional structural geometries are also different. The Andean fold-thrust belt is characterized by multiple linked contractional structures defining ramp-flat geometries above décollement levels along the basement-cover interface or within Phanerozoic cover strata. In contrast, intraforeland structures are delineated by solitary basement-involved reverse faults that generate discrete topographic highs or broad arches that are topographically disconnected from the Andes.

STRATIGRAPHIC FRAMEWORK

The Phanerozoic stratigraphic package of western South America shows variability in the distribution and thickness of Andean and pre-Andean basin fill (Fig. 3). Cenozoic nonmarine strata accumulated during widespread Andean orogenesis involving thrust-belt development, crustal loading, and flexural subsidence that produced a contiguous foreland basin containing ~2–6 km of clastic fill (Horton, 2018b). Pre-Andean sedimentation comprised marine and nonmarine deposition in separate Paleozoic and Mesozoic basins, including multiple extensional basins succeeded by post-extensional sags governed by thermal subsidence. This heterogeneous depositional history led to regional disparities in stratigraphic framework (Fig. 3).

Along the western margin, ~10 long-lived basement arches exhibit sharply reduced stratigraphic thicknesses (Fig. 3). These basement highs compartmentalize pre-Cenozoic depocenters that helped guide Andean strain localization. For example, the anomalously thick (>6–12 km), eastward-tapering Paleozoic succession in Bolivia coincides with the widest part of the fold-thrust belt (Fig. 2, profile 5), where the thrust front reaches a position 700–900 km from the trench. Mesozoic extensional basins were also selectively inverted, with Andean reactivation of former normal faults as contrac-

[1]Supplemental Material. Methods and structural and topographic data for regional profiles. Please visit https://doi.org/10.1130/GEOL.S.19783087 to access the supplemental material, and contact editing@geosociety.org with any questions.

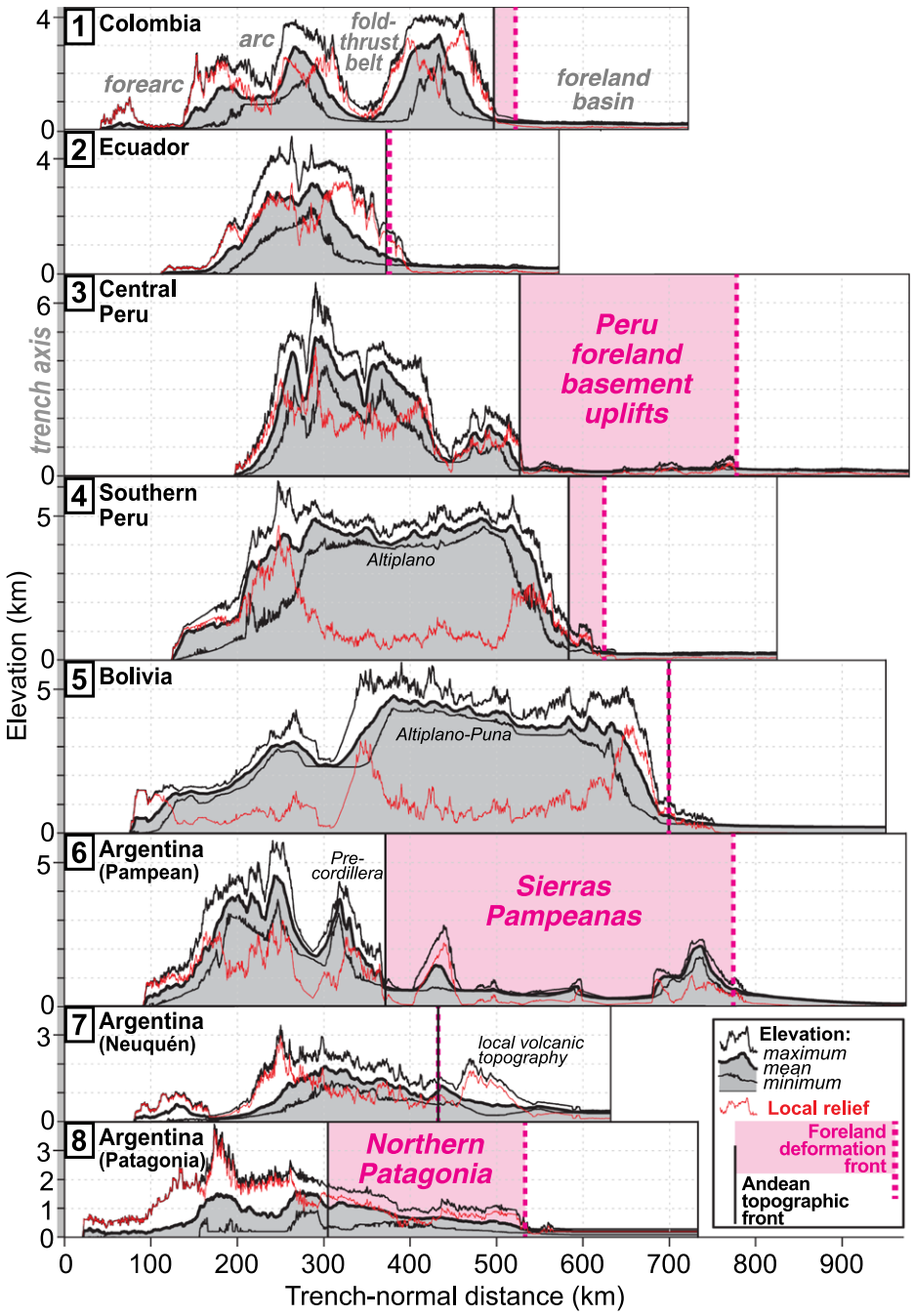

Figure 2. Representative trench-normal profiles showing swath-averaged topography (minimum, maximum, and mean elevation; black lines), relief (red line), and the traces of the Andean topographic front (black vertical line) and foreland deformation front (pink vertical dashed line). Pink shading shows zones where the foreland deformation front is situated far inboard of the Andean mountain front.

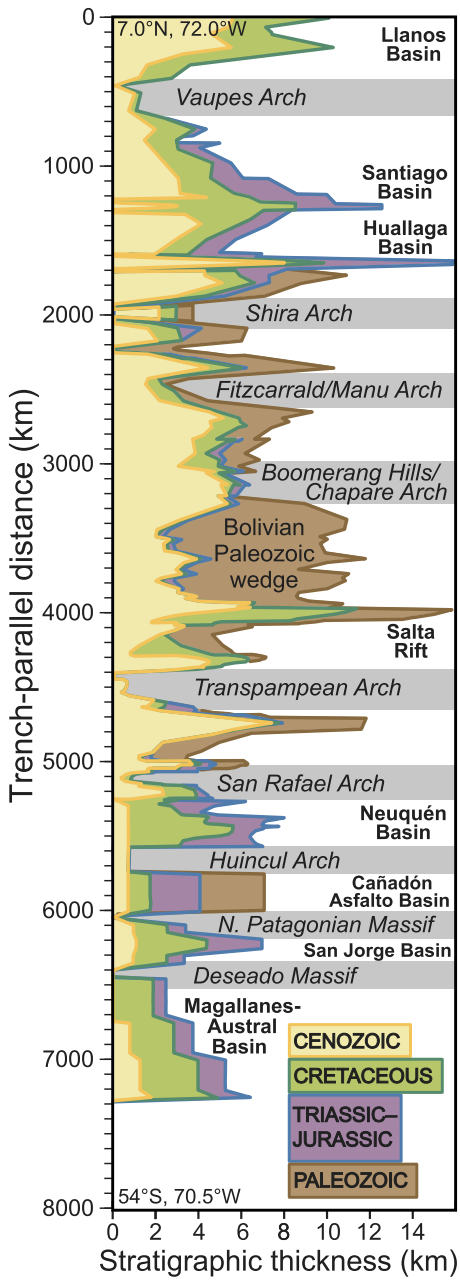

Figure 3. Plot of Phanerozoic stratigraphic thicknesses along the Andean topographic front and proximal foreland region of western South America (modified from McGroder et al., 2015). Note the diminished cumulative thicknesses over a series of Precambrian basement highs (gray shading).

tional structures (McGroder et al., 2015; Perez et al., 2016).

The spatially restricted pre-Andean depocenters are co-located with younger "thin-skinned" fold-thrust systems above décollements localized by mechanical anisotropies within Paleozoic–Mesozoic strata or along the basement-cover interface (Kley et al., 1999; McQuarrie, 2002). This correlation of precursor basin geometry with structural style highlights the influence of the inherited stratigraphic architecture on the mode and magnitude of deformation advance.

OCEAN-CONTINENT PLATE INTERACTIONS

Subduction of seismic and aseismic ridges provides opportunities for assessing the role of flat slab subduction and slab window development in promoting or inhibiting retroarc deformation advance. The response of the overriding plate can be evaluated by considering the orthogonal distances from the trench to the (1) Andean topographic front, and (2) foreland deformation front (Fig. 1) along the ~8000 km orogenic length (Fig. 4). These two features show large variations. From 10°N to 55°S, three zones of substantial deformation advance coincide with the Peruvian and Pampean foreland provinces of flat slab subduction and the Chile Ridge subduction region (Fig. 4A). A fourth prominent zone of inboard deformation involves the thick Paleozoic stratigraphic

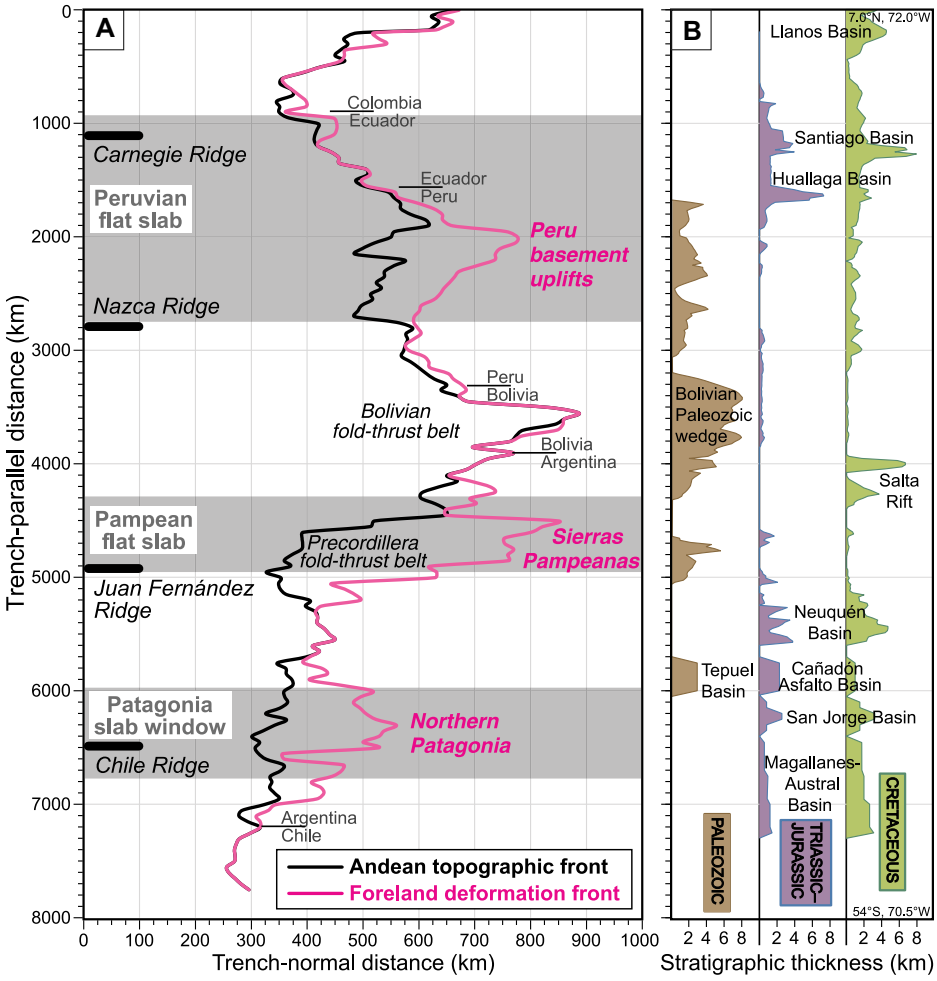

Figure 4. Plots showing along-strike variations in the Andean topographic front and foreland deformation front (A), with distinct foreland zones of distributed basement deformation (gray shading), and stratigraphic architecture along the South American margin (B). Note the position of basin depocenters relative to the Andean topographic front.

package of the Bolivian Andes (17°S –23°S) (Fig. 4B).

These four maxima in the position of the deformational front (Fig. 4A) highlight several spatial relationships. First, flat slab subduction and ridge subduction are spatially associated with large-magnitude deformation advance, highlighting the importance of the geodynamic configuration of the subducting plate—specifically, the subduction of aseismic ridges that promote flat slab subduction and active ridges that induce slab window opening. Second, the inherited pre-Andean stratigraphic framework (Fig. 4B) also relates to deformation advance, with the exceptionally wide fold-thrust belt in Bolivia (where the mountain front coincides with the deformation front; Fig. 2) corresponding to the position of the thick, eastward-tapering Paleozoic stratigraphic wedge. Triassic–Jurassic extensional depocenters preferentially coincide with narrow orogenic segments of the northern and southern Andes (Fig. 4B), possibly due to stalled deformation advance in which basin inversion occurs through reactivation of weak, preexisting extensional structures in westernmost retroarc regions.

DISCUSSION

Deformation Advance and Intraforeland Shortening

Increased deformation advance in South America is spatially correlated with inherited stratigraphic geometries, ridge subduction, and flat slab subduction. The maximum inboard position of the Andean thrust front coincides with a thick Paleozoic stratigraphic wedge restricted to Bolivia (17°S –23°S) (Fig. 3), where mechanical anisotropies are prone to failure and propagation of thin-skinned shortening (Kley et al., 1999; McQuarrie, 2002). This region was also preconditioned by early Cenozoic flat slab subduction (Ramos and Folguera, 2009; Perez and Levine, 2020; Runyon et al., 2022; Sundell et al., 2022), which may have induced thermal or strain weakening. Alternatively, the Bolivian orocline and corresponding trench curvature may be linked to the large width of the subducted slab and along-strike changes in slab retreat relative to overriding plate motion (Schellart, 2017; Schellart and Strak, 2021). Elsewhere, the positions of the Andean thrust front and intraforeland uplifts coincide with pre-Andean structural or stratigraphic discontinuities (McGroder et al., 2015). Many foreland structures are reactivated features, underscoring the influence of inherited crustal rheology and associated heterogeneities.

The foreland deformation front may penetrate far into the low-relief foreland basin, as much as 400 km inboard of the Andean mountain front (Fig. 2). Intraforeland uplifts in northern Patagonia (45°S –48°S) broadly match the intersection of the Chile Ridge and Mocha fracture zone with the margin, suggesting that slab window development has focused inboard deformation (Ramos, 2005; Orts et al., 2021), potentially due to thermal weakening of a region with limited sedimentary cover. In contrast, isolated basement uplifts of the Peruvian and Pampean segments correspond to zones of flat slab subduction (Fig. 4). These dissimilar settings demonstrate that Andean foreland uplifts can rarely be attributed to a single mechanism.

Flat Slab Subduction

The spatial overlap of flat slab subduction with intraplate deformation raises questions regarding the cause of shortening far from the trench. Although commonly posed as a debate between basal traction and end loading along the plate interface (Bird, 1984; Axen et al., 2018), we offer two points. First, the thermal effects of shallow subduction are not limited to the forearc (Dumitru et al., 1991) but involve abrupt refrigeration and hence increased strength above the entire flat slab (Gutscher et al., 2000). Such strengthening would enable long-distance stress transmission. Second, enhanced input of slab-derived hydrous fluids weakens selected foreland regions (Saylor et al., 2020). Such fluid-induced weakening may be maximized above the leading slab hinge at the transition from the flat segment to deeper steep segment.

These strengthening and weakening processes operate simultaneously in different sectors. Regionally, cooling due to flat slab subduction inhibits uniform deformation and promotes stress transmission along the subhorizontal interplate contact and within overriding lithosphere. Separately, toward the plate interior, heightened fluid influx and lithospheric weakening focused above the slab hinge facilitate activation of isolated basement structures that overlie bulldozed continental material at depth.

Drivers of Intraforeland Deformation

The correlation of flat slab subduction with pronounced deformation advance (Figs. 1 and 4) demonstrates the importance of shallow subduction in driving deformation in the Andean fore-

land. However, flat slab subduction should not be considered necessary or sufficient because inherited structures and stratigraphic architecture (Figs. 3 and 4) have also guided deformation in the thrust belt and foreland. Although less appreciated, ocean ridge subduction and slab window development also may be linked to intraforeland deformation.

By analogy with the Andes, episodes of intraplate deformation in other noncollisional systems may involve comparable catalysts. Whereas flat slab subduction and tectonic inheritance are well established for continental interiors (Ye et al., 1996; Li and Li, 2007; Yonkee and Weil, 2015; Kusky et al., 2016), ridge subduction offers a further alternative that could be identified by shifts in magmatism, metamorphism, and hydrothermal activity (Bradley et al., 2003).

CONCLUSIONS

Deformation advance in South America is assessed through delineation of the Andean topographic front and foreland deformation front. The correlation of flat slab subduction and ridge subduction with intraplate basement uplift demonstrates a link between subduction geometry and retroarc shortening. However, shallow subduction is neither necessary nor sufficient to uniquely explain the inboard advance of deformation within continental plate interiors. We suggest that inherited properties of the overriding plate, such as preexisting structural and stratigraphic anisotropies and time-dependent thermal and rheological properties, are critical for strain localization in the thrust belt and adjacent foreland. As the type example of Cordilleran orogenesis, the Andes offer insights into how tectonic inheritance, subduction dynamics, and crustal or lithospheric strengthening and weakening influence the structure and topography of convergent plate boundaries.

ACKNOWLEDGMENTS

This work was supported by U.S. National Science Foundation grants EAR-1918541 and EAR-1925898. Comments from A. Folguera, J. Saylor, V. Strak, and an anonymous reviewer improved the manuscript.

REFERENCES CITED

Axen, G.J., van Wijk, J.W., and Currie, C.A., 2018, Basal continental mantle lithosphere displaced by flat-slab subduction: Nature Geoscience, v. 11, p. 961–964, https://doi.org/10.1038/s41561-018-0263-9.

Bishop, B.T., Beck, S.L., Zandt, G., Wagner, L.S., Long, M.D., and Tavera, H., 2018, Foreland uplift during flat subduction: Insights from the Peruvian Andes and Fitzcarrald Arch: Tectonophysics, v. 731–732, p. 73–84, https://doi.org/10.1016/j.tecto.2018.03.005.

Bird, P., 1984, Formation of the Rocky Mountains foreland and Great Plains: Tectonics, v. 3, p. 741–758, https://doi.org/10.1029/TC003i007p00741.

Bradley, D., Kusky, T., Haeussler, P., Goldfarb, R., Miller, M., Dumoulin, J., Nelson, S.W., and Karl, S., 2003, Geologic signature of early Tertiary ridge subduction in Alaska, *in* Sisson, V.B., et al., eds., Geology of a Transpressional Orogen Developed during Ridge-Trench Interaction along the North Pacific Margin: Geological Society of America Special Paper 371, p. 19–49, https://doi.org/10.1130/0-8137-2371-X.19.

Breitsprecher, K., and Thorkelson, D.J., 2008, Neogene kinematic history of Nazca-Antarctic-Phoenix slab windows beneath Patagonia and the Antarctic Peninsula: Tectonophysics, v. 464, p. 10–20, https://doi.org/10.1016/j.tecto.2008.02.013.

Capaldi, T.N., McKenzie, N.R., Horton, B.K., Mackaman-Lofland, C., Colleps, C.L., and Stockli, D.F., 2021, Detrital zircon record of Phanerozoic magmatism in the southern Central Andes: Geosphere, v. 17, p. 876–897, https://doi.org/10.1130/GES02346.1.

Costa, C., et al., 2020, Hazardous faults of South America: Compilation and overview: Journal of South American Earth Sciences, v. 104, 102837, https://doi.org/10.1016/j.jsames.2020.102837.

Dickinson, W.R., and Snyder, W.S., 1978, Plate tectonics of the Laramide orogeny, *in* Matthews, V., III, ed., Laramide Folding Associated with Basement Block Faulting in the Western United States: Geological Society of America Memoir 151, p. 355–366, https://doi.org/10.1130/MEM151-p355.

Dumitru, T.A., Gans, P.B., Foster, D.A., and Miller, E.L., 1991, Refrigeration of the western Cordilleran lithosphere during Laramide shallow-angle subduction: Geology, v. 19, p. 1145–1148, https://doi.org/10.1130/0091-7613(1991)019<1145:ROTWCL>2.3.CO;2.

Gautheron, C., Espurt, N., Barbarand, J., Roddaz, M., Baby, P., Brusset, S., Tassan-Got, L., and Douville, E., 2013, Direct dating of thick- and thin-skin thrusts in the Peruvian Subandean zone through apatite (U-Th)/He and fission track thermochronometry: Basin Research, v. 25, p. 419–435, https://doi.org/10.1111/bre.12012.

Gutscher, M.-A., Spakman, W., Bijwaard, H., and Engdahl, E.R., 2000, Geodynamics of flat subduction: Seismicity and tomographic constraints from the Andean margin: Tectonics, v. 19, p. 814–833, https://doi.org/10.1029/1999TC001152.

Horton, B.K., 2018a, Tectonic regimes of the central and southern Andes: Responses to variations in plate coupling during subduction: Tectonics, v. 37, p. 402–429, https://doi.org/10.1002/2017TC004624.

Horton, B.K., 2018b, Sedimentary record of Andean mountain building: Earth-Science Reviews, v. 178, p. 279–309, https://doi.org/10.1016/j.earscirev.2017.11.025.

Jordan, T.E., Isacks, B.L., Allmendinger, R.W., Brewer, J.A., Ramos, V.A., and Ando, C.J., 1983, Andean tectonics related to geometry of subducted Nazca plate: Geological Society of America Bulletin, v. 94, p. 341–361, https://doi.org/10.1130/0016-7606(1983)94<341:ATRTGO>2.0.CO;2.

Kley, J., Monaldi, C.R., and Salfity, J.A., 1999, Along-strike segmentation of the Andean foreland: Causes and consequences: Tectonophysics, v. 301, p. 75–94, https://doi.org/10.1016/S0040-1951(98)90223-2.

Kusky, M.T., Windley, F.B., Wang, L., Wang, Z.S., Li, X.Y., and Zhu, P.M., 2014, Flat slab subduction, trench suction, and craton destruction: Comparison of the North China, Wyoming, and Brazilian cratons: Tectonophysics, v. 630, p. 208–221, https://doi.org/10.1016/j.tecto.2014.05.028.

Kusky, T.M., et al., 2016, Insights into the tectonic evolution of the North China Craton through comparative tectonic analysis: A record of outward growth of Precambrian continents: Earth-Science Reviews, v. 162, p. 387–432, https://doi.org/10.1016/j.earscirev.2016.09.002.

Li, Z.X., and Li, X.H., 2007, Formation of the 1300-km-wide intracontinental orogen and postorogenic magmatic province in Mesozoic South China: A flat-slab subduction model: Geology, v. 35, p. 179–182, https://doi.org/10.1130/G23193A.1.

McGroder, M.F., Lease, R.O., and Pearson, D.M., 2015, Along-strike variation in structural styles and hydrocarbon occurrences, Subandean fold-and-thrust belt and inner foreland, Colombia to Argentina, *in* DeCelles, P.G., et al., eds., Geodynamics of a Cordilleran Orogenic System: The Central Andes of Argentina and Northern Chile: Geological Society of America Memoir 212, p. 79–113, https://doi.org/10.1130/2015.1212(05).

McQuarrie, N., 2002, Initial plate geometry, shortening variations, and evolution of the Bolivian orocline: Geology, v. 30, p. 867–870, https://doi.org/10.1130/0091-7613(2002)030<0867:IPGSVA>2.0.CO;2.

Orts, D.L., Álvarez, O., Zaffarana, C., Gimenez, M., Ruiz, F., and Folguera, A., 2021, Tectonic segmentation across Patagonia controlled by the subduction of oceanic fracture zones: Journal of Geodynamics, v. 143, 101806, https://doi.org/10.1016/j.jog.2020.101806.

Perez, N.D., and Levine, K.G., 2020, Diagnosing an ancient shallow-angle subduction event from Cenozoic depositional and deformational records in the central Andes of southern Peru: Earth and Planetary Science Letters, v. 541, 116263, https://doi.org/10.1016/j.epsl.2020.116263.

Perez, N.D., Horton, B.K., and Carlotto, V., 2016, Structural inheritance and selective reactivation in the central Andes: Cenozoic deformation guided by pre-Andean structures in southern Peru: Tectonophysics, v. 671, p. 264–280, https://doi.org/10.1016/j.tecto.2015.12.031.

Proyecto Multinacional Andino, 2009, Atlas de deformaciones cuaternarias de Los Andes: Servicio Nacional de Geológia y Minería Publicacion Geológica Multinacional 7, 311 p.

Ramos, V.A., 2005, Seismic ridge subduction and topography: Foreland deformation in the Patagonian Andes: Tectonophysics, v. 399, p. 73–86, https://doi.org/10.1016/j.tecto.2004.12.016.

Ramos, V.A., and Folguera, A., 2009, Andean flat-slab subduction through time, *in* Murphy, J.B., et al., eds., Ancient Orogens and Modern Analogues: Geological Society, London, Special Publication 327, p. 31–54, https://doi.org/10.1144/SP327.3.

Ramos, V.A., Cristallini, E.O., and Pérez, D.J., 2002, The Pampean flat-slab of the Central Andes: Journal of South American Earth Sciences, v. 15, p. 59–78, https://doi.org/10.1016/S0895-9811(02)00006-8.

Runyon, B., Saylor, J.E., Horton, B.K., Reynolds, J.H., and Hampton, B., 2022, Basin evolution in response to flat subduction in the Altiplano: Journal of the Geological Society, v. 179, jgs2021-003, https://doi.org/10.1144/jgs2021-003.

Saylor, J.E., Rudolph, K.W., Sundell, K.E., and van Wijk, J., 2020, Laramide orogenesis driven by Late Cretaceous weakening of the North American lithosphere: Journal of Geophysical Research, v. 125, e2020JB019570, https://doi.org/10.1029/2020JB019570.

Schellart, W.P., 2017, Andean mountain building and magmatic arc migration driven by subduction-induced whole mantle flow: Nature Communications, v. 8, 2010, https://doi.org/10.1038/s41467-017-01847-z.

Schellart, W.P., and Strak, V., 2021, Geodynamic models of short lived, long-lived and periodic flat slab subduction: Geophysical Journal International, v. 226, p. 1517–1541, https://doi.org/10.1093/gji/ggab126.
Styron, R., and Pagani, M., 2020, The GEM global active faults database: Earthquake Spectra, v. 36, p. 160–180, https://doi.org/10.1177/8755293020944182.
Sundell, K.E., George, S.W.M., Carrapa, B., Gehrels, G.E., Ducea, M.N., Saylor, J.E., and Pepper, M., 2022, Crustal thickening of the northern Central Andean Plateau inferred from trace elements in zircon: Geophysical Research Letters, v. 49, e2021GL096443, https://doi.org/10.1029/2021GL096443.
Ye, H.Z., Royden, L., Burchfiel, C., and Schuepbach, M., 1996, Late Paleozoic deformation of interior North America: The greater Ancestral Rocky Mountains: The American Association of Petroleum Geologists Bulletin, v. 80, p. 1397–1432, https://doi.org/10.1306/64ED9A4C-1724-11D7-8645000102C1865D.
Yonkee, W.A., and Weil, A.B., 2015, Tectonic evolution of the Sevier and Laramide belts within the North American Cordillera orogenic system: Earth-Science Reviews, v. 150, p. 531–593, https://doi.org/10.1016/j.earscirev.2015.08.001.

Printed in USA